S/V measurements in a ^{3}He bead phantom using a short-time-scale NMR diffusion sequence

M. Carl[1], G. W. Miller[2], J. P. Mugler III[2], W. A. Tobias[1], and G. D. Cates[1,2]

[1]Physics, University of Virginia, Charlottesville, VA, United States, [2]Radiology, University of Virginia, Charlottesville, VA, United States

Introduction/Purpose: Hyperpolarized ^{3}He diffusion NMR is a powerful tool to probe lung microstructure at short length scales inaccessible by conventional *k*-space MRI. For a short diffusion time Δ, time-dependent diffusion measurements are sensitive to the surface-to-volume ratio (*S/V*) of the surrounding structure [1]. Because of the high gas diffusivity (D_{Xe}=0.14cm^2/s and D_{He}=0.88cm^2/s in air) and the small size of alveoli (~200μm), measurement of *S/V* with the conventional single bipolar diffusion technique has not been feasible in the lung since only weak diffusion attenuation can be imparted within the short-time-scale regime (~200μs for D_{Xe}). In previous work we described a method to perform short-time-scale hyperpolarized gas diffusion measurements and tested it in a one inch spherical ^{3}He phantom [2]. In the present work we use this technique to measure S/V in a more challenging regime closer to the actual lung microstructure.

Methods: S/V measurements were performed using a 3mm bead-pack phantom (similar to Ref.[3]) filled with ~2atm of thermally-polarized ^{3}He and ~1atm of O_2. The bead compartment of the phantom is connected on one side to a bead-free chamber, which enabled us to obtain a reliable measure of D_0. Diffusion measurements obtained using the pulse sequence described below were made at diffusion times ranging from Δ = 400μs to 1000μs, and were used to calculate *S/V* of the pore space between the beads. All NMR measurements were performed using a commercial 1.5T scanner (Siemens Sonata) equipped with a homebuilt ^{3}He birdcage RF coil.

The basis of our pulse sequence (Fig.1) is to concatenate many bipolar diffusion gradients ("unit cells") to increase the diffusion weighting ($b_{total} \rightarrow Nb$). To compensate for the susceptibility-induced short T_2* relaxation time (~1.1ms) within the bead chamber, we employed periodic RF refocusing pulses to prolong the useable signal duration. In contrast to the standard spin-echo diffusion sequence, refocusing pulses were only applied between complete bipolar gradient pairs in order to preserve the fundamentally short diffusion times. Phase-cycled averaging was used to cancel any spurious echoes that would otherwise contaminate the measurements. In addition to diffusion-attenuated signal measurements, reference scans, with all gradients turned off, were acquired. The diffusion-attenuated signal was divided by the reference signal to normalize for T_2* decay. The ratio of the diffusion-attenuated to reference signal at the end of the n^{th} unit cell corresponds to: $R(n) = \exp(-nbD)$. For every unit cell, we take the signal ratio during the following wait-time (see Fig.1) and assign its average value to $R(n)$, so that a fit of $\ln[R(n)]$ vs. n yields D.

As described in Ref.[2], the wait time, T_{wait}, that is inserted between consecutive unit cells, which are applied along orthogonal axes, allows the edge effect in a given direction to diffuse away while diffusion weighting is imparted along orthogonal axes. The effective wait time between gradients along the same axis is referred to as the equilibrium time, T_{eq}. In order to derive a semi-analytic criterion to minimize the edge effect distortions [2], we also simulated the multiple bipolar gradient sequence for restricted diffusion as a function of T_{eq} using several diffusion times (Δ), diffusion constants (D_0) and various geometrical shapes and sizes (S/V).

Results: A representative plot of averaged experimental signal data (Δ = 400μs) from the bead-pack region of the phantom is shown in Fig.2a. The blue curve is the periodically-refocused reference curve, and the red curve is the signal evolution during and between the bipolar gradient waveforms. Fig.2b shows the corresponding ratio $R(n)$. The red line represents the exponential fit, which allows the calculation of D.

To minimize any edge effect distortions, we found that the simulated diffusivity asymptotically approaches the correct value as a function of the unit-less quantity $\eta = T_{eq}*\mathrm{sqrt}((S/V)^2*D_0/\Delta)$. Fig.3 shows the dependence of the simulated apparent diffusion constant (normalized to one) for different Δ, S/V and D_0 values as a function of η. As one can observe, the asymptotic approach agrees rather well for the different configurations.

Fig.4 shows experimentally measured diffusion constants using the sequence shown in Fig.1 plotted as a function of √Δ. From the slope, one can determine *S/V*. We found that the experimental *S/V* was 35 ± 3 cm^{-1}. Assuming that we know the surface to volume of our phantom within 10%, this result is in good agreement with the expected value of 31.3 ± 3.1 cm^{-1}.

Conclusion/Outlook: We have developed and optimized a robust method for measuring diffusivities at very short diffusion times, which represents a crucial step toward enabling the extraction of *S/V* in the lung microstructure. Because of the short T_2* within the bead phantom, we modified our original sequence to include periodic 180° refocusing RF pulses to extend the lifetime of the signal and hence the possible number of diffusion gradient pairs. Through simulations, we found that the required equilibrium time can be combined with other relevant parameters into a unit-less quantity η, which describes the asymptotic approach of the diffusivity to its correct value. Experimental results demonstrate that, in the short-time-scale regime, our sequence is capable of determining $D(\Delta)$ and hence S/V in an environment that is even more hostile (extremely short T_2*) than the in vivo lung. In future experiments, we will test our sequence in glass bead packs with a smaller bead diameter and finally in vivo using hyperpolarized ^{129}Xe.

References: [1] Mitra et al, Phys. Rev. B47, No. 14, (1993) [2] Carl et. al, J. Magn. Reson. 189 (2007) 228-240 [3] Mair et. al, Phys. Rev. Lett. 83, (1999) 3324-3327

Acknowledgments: Research supported by NIH grant R01 HL079077 and Siemens Medical Solutions.

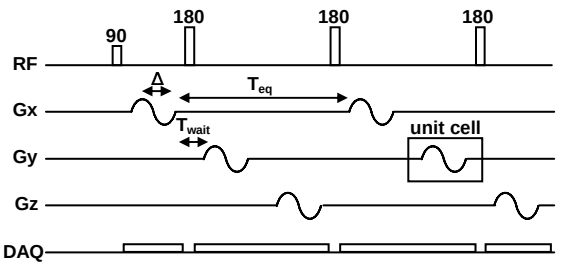

Fig1: Multiple bipolar pulse sequence.

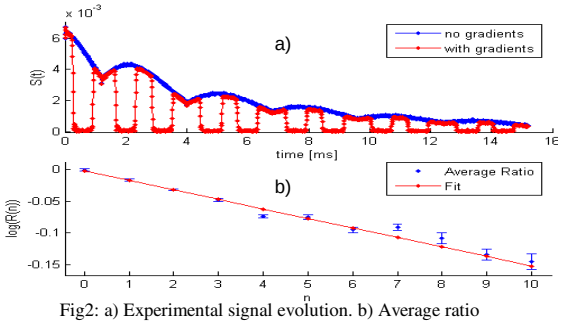

Fig2: a) Experimental signal evolution. b) Average ratio

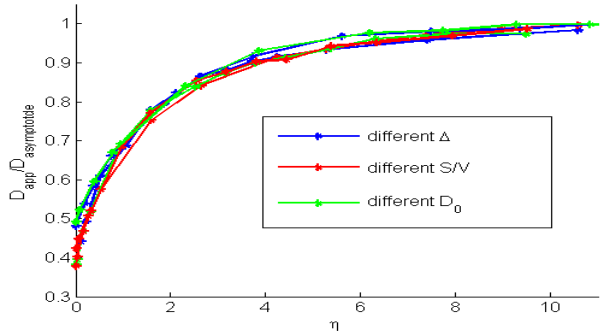

Fig3: Approach of the diffusivity to its correct asymptote.

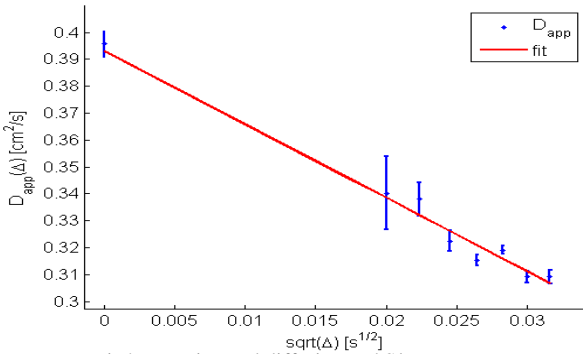

Fig4: Experimental diffusion and S/V measurements.